

Shifts in plankton size spectra modulate growth and coexistence of anchovy and sardine in upwelling systems¹

T. Mariella Canales, Richard Law, and Julia L. Blanchard

Abstract: Fluctuations in the abundance of anchovy (*Engraulis* spp.) and sardine (*Sardinops sagax*) are widespread in marine ecosystems, but the causes still remain uncertain. Differences between the planktonic prey availability, selectivity, and predation between anchovy and sardine have been suggested as factors influencing their dynamics. Using a dynamical multispecies size-spectrum model, we explore the consequences of changes in plankton size composition, together with intraguild predation and cannibalism, on the coexistence of these species. The shift towards smaller plankton has led to a reduction in the growth rate of both species. The effect was more deleterious on anchovy growth because it is unable to filter small particles. In model scenarios that included the effects of cannibalism and predation, anchovy typically collapsed under conditions favouring smaller sized plankton. The two species coexisted under conditions of larger sized plankton, although strong predation in conjunction with weak cannibalism led to the loss of sardine. The model provides new testable predictions for the consequences of plankton size structure on anchovy and sardine fluctuations. Further empirical work is needed to test these predictions in the context of climate change.

Résumé : Si des fluctuations de l'abondance des anchois (*Engraulis* spp.) et des sardines (*Sardinops sagax*) sont répandues dans les écosystèmes marins, leurs causes demeurent mal comprises. Des différences sur le plan de la disponibilité de proies planctoniques, de la sélectivité et de la prédation entre les anchois et les sardines ont été proposées comme étant des facteurs qui influencent leur dynamique. À l'aide d'un modèle de spectre de tailles multiespèces dynamique, nous examinons les conséquences de changements à la composition selon la taille du plancton, ainsi que de la prédation intragilde et du cannibalisme, sur la coexistence de ces espèces. La diminution de la taille du plancton entraîne une réduction des taux de croissance des deux espèces. Cet effet est plus délétère pour la croissance des anchois parce que ces dernières sont incapables de filtrer les petites particules. Dans les scénarios modélisés comprenant les effets du cannibalisme et de la prédation, l'effondrement des anchois est typiquement observé dans des conditions favorisant le plancton de plus petite taille. Les deux espèces coexistent dans des conditions de plancton de plus grande taille, bien qu'une forte prédation combinée à un faible cannibalisme mène à la disparition de sardines. Le modèle fournit de nouvelles prédictions vérifiables concernant les conséquences de la structure selon la taille du plancton sur les fluctuations de l'abondance des anchois et des sardines. D'autres travaux empiriques sont nécessaires pour valider ces prédictions dans un contexte de changements climatiques. [Traduit par la Rédaction]

Introduction

Large fluctuations of anchovy (*Engraulis* spp.) and sardine (*Sardinops sagax*) are a well-known feature in the productive coastal waters of the northwestern, northeastern, and southeastern Pacific and in the southeastern Atlantic (Lluch-Belda et al. 1989; Schwartzlose et al. 1999). California, Humboldt, Benguela, and Canary systems form the Eastern Upwelling Marine Ecosystems (EBUEs) that are among the most productive marine ecosystems of the world, providing about one-fifth of the global marine fish catch and contributing to food security and livelihoods. Within the EBUEs, the Humboldt Current System (HCS) makes the highest contribution in catch to the fish production mainly due to *Engraulis ringens* (Fréon et al. 2009). It is therefore important to understand how these ecosystems work, both for economic and for scientific reasons.

Many different oceanographic drivers have been proposed to influence sardine and anchovy fluctuations (MacCall 2009). For example, Chavez et al. (2003) linked the anchovy and sardine fluctua-

tions to the large-scale variability in temperature, carbon dioxide concentration, and coastal and ocean productivity. MacCall (2002) identified the flow in boundary current as the unifying feature associated with worldwide fluctuations of small pelagic fish. Takasuka et al. (2007) found an "optimal growth temperature," noting that larval growth is maximised at a higher temperature in anchovy than in sardine. Bertrand et al. (2011) proposed that near-surface oxygen concentration/saturation levels explain sardine and anchovy distributions. Mechanisms such as natal homing, school-mixing, and the "loop-hole hypothesis" have also been proposed as ways in which the populations recover from deleterious conditions (Cury 1994; Bakun and Cury 1999; Bakun 2001; Bertrand et al. 2004).

Size-dependent food web processes may also play an important role in concert with the environment. van der Lingen et al. (2006) provided evidence that both species are trophically distinct, with sardine feeding on smaller particles than anchovy. Intraguild predation (IGP) through predation of larger individuals on smaller ones was recently suggested to amplify small changes in anchovy

Received 4 April 2015. Accepted 17 October 2015.

Paper handled by Associate Editor Julia Baum.

T.M. Canales. Center of Applied Ecology and Sustainability (CAPES), Pontificia Universidad Católica de Chile, Av. Alameda 340, Santiago, Chile.

R. Law. The University of York, York Centre for Complex Systems Analysis, Ron Cooke Hub, York, YO10 5EG, United Kingdom.

J.L. Blanchard. University of Tasmania, Institute of Marine and Antarctic Studies, Hobart, 20 Castray Esplanade, Battery Point TAS 7004, Australia.

Corresponding author: T. Mariella Canales (email: mariella.canales@gmail.com).

¹This article is part of a special issue entitled "Size-based approaches in aquatic ecology and fisheries science: a symposium in honour of Rob Peters".

Table 1. Body size of the fish size spectra and parameters of the plankton spectra.

Symbol	Parameter description	Value(s)	Unit	Source
$(x_{a,\min}, x_{a,\max})$	Minimum and maximum anchovy body sizes	(-8.2, 4.2)		
$(x_{s,\min}, x_{s,\max})$	Minimum and maximum sardine body sizes	(-5.7, 6.4)		
U_{p,x_0}	Numerical density of plankton at x_0 ; cool conditions	$e^{24.25}$	m^{-3}	Braun et al. 2009
λ_p	Slope of the plankton spectrum; cool conditions	-1.26		
U_{p,x_0}	Numerical density of plankton at x_0 ; warm conditions	$e^{25.36}$	m^{-3}	
λ_p	Slope of plankton spectrum; warm conditions	-1.63		

Note: $x = \ln(w/w_0)$, where w is body mass and $w_0 = 1$ g.

and sardine abundance generated by the environment (Irigoin and de Roos 2011) along with its synergism with cannibalism (Valdés-Szeinfeld 1991). Because the effects of the physical environment are modulated by the physiology and behavior of individuals, the dynamics of populations, ecosystem-level changes in productivity and trophic interactions (Rijnsdorp et al. 2009), and fishing effects (Essington et al. 2015), it can be difficult to tease the main drivers apart.

In this study, we focus on the relative roles of size-dependent prey availability, selectivity, and intraguild predation on the dynamical behavior of sardine and anchovy using a multispecies size-spectrum model. Under simplified model scenarios, we show that a shift in planktonic prey size composition can affect growth and vulnerability to predation and, therefore, the coexistence of anchovy and sardine. Anchovy experienced a greater loss in somatic growth under smaller sized plankton than sardine due to differences in their feeding mechanisms (e.g., gape diameter, gill raker gap, and types). Cannibalism and intraguild predation amplified the effects of this difference, causing loss of anchovy under reduced plankton size composition, but both species coexisted when larger plankton were present.

Methods

We used a size-based version of the McKendrick – von Foerster equation (McKendrick 1926) to describe the dynamics of a pelagic ecosystem comprising two dynamic spectra, anchovy (a) and sardine (s), supported by a fixed plankton spectrum (p). Such models draw on the strong observed size structuring of marine ecosystems (Sheldon et al. 1972) and are increasingly used to describe the dynamics of size-dependent, multispecies, feeding interactions (Andersen and Beyer 2006; Hartvig et al. 2011; Hartvig and Andersen 2013; Blanchard et al. 2014). The models explicitly do the bookkeeping of biomass in an ecosystem through fish eating other organisms and increasing in body mass. Thus, they allow the direct effect of changes in the plankton spectrum on growth to be modelled. Also, fish die partly because they are eaten: they are not fixed to an external mortality rate so far as predation is concerned.

The primary state variables are density functions $N_i(w, t)$ ($g^{-1} \cdot m^{-3}$) at time t for anchovy and sardine ($i \in \{a, s\}$) at body mass w . Note that the plankton spectrum was held fixed at values estimated for cool and warm conditions to ensure that the direct effect on fish growth of the two plankton states could be examined. Size spectra extend over many orders of magnitude, and we therefore used density functions $U_i(x, t)$ (m^{-3}) in log-transformed body mass x , where $w = w_0 \exp(x)$, with $w_0 = 1$ g here. Size ranges covered by the spectra are given in Table 1. Appendix A describes the details of the model, and Appendix B gives parameter values and their sources.

To describe the dynamics of anchovy and sardine in upwelling systems requires two changes from previous size-spectrum models: (1) a plankton spectrum that differs in size structure depending on whether conditions are warm or cool, and (2) a feeding kernel that takes into account the planktivorous feeding of the two species. These differences are explained below.

Size-structures of the plankton community

Observed plankton size spectra have been shown to shift towards smaller sizes under warmer temperatures (Barnes et al. 2011). To

capture the relative differences in plankton size composition that have been observed under cool (non-El Niño/La Vieja) and warm (El Niño/El Viejo) conditions, two contrasting, fixed plankton size spectra were used.

We used directly observed plankton spectrum data combined with an empirical method for determining phytoplankton community size structure from satellite data (Barnes et al. 2011) to approximate these two contrasting plankton size spectrum conditions.

Plankton data were obtained from a monitoring survey carried out in October 2008 in the Northern Chilean Marine Ecosystem (NCME) ($18^{\circ}21'S-24^{\circ}00'S$) (Braun et al. 2009), as described in Appendix C. The survey encompassed a size range from picoplankton (cell mass of 7×10^{-13} g) up to zooplankton (cell mass of 0.1 g), with the largest phytoplankton being close to 10^{-7} g. From the survey, we estimated two parameters of the plankton size spectrum, slope (λ_p) and density U_{p,x_0} at smallest body mass $\exp(x_0) = 10^{-10}$ g consumed by fish. The estimated value of $U_{p,x_0} = 4.7 \times 10^{10} m^{-3}$ resulted in somatic growth for anchovy and sardine in the size-spectrum model slower than in the literature-based von Bertalanffy growth of these species. We therefore used a greater value $U_{p,x_0} = 3.4 \times 10^{11} m^{-3}$ (Table 1) to generate growth trajectories close to those of the von Bertalanffy growth equations previously estimated for the species (Canales and Leal 2009). The survey was carried out under cool conditions, which should be good for anchovy growth (van der Lingen et al. 2006), and the value lay within the 95% confidence interval of the predicted density at the smallest body mass 10^{-10} g for the plankton size spectrum described in Appendix C.

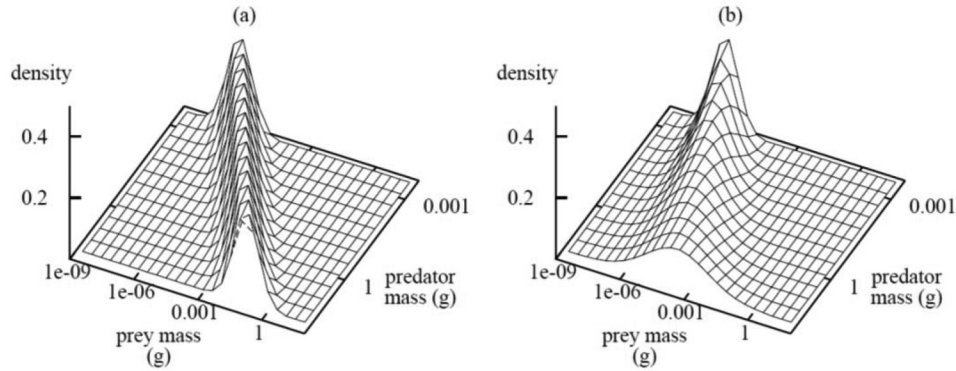
To approximate the plankton size composition under warm conditions, chlorophyll *a* (CHL) was obtained from the satellite-borne Sea-viewing Wide Field-of-view Sensor (SeaWiFS; <http://oceancolor.gsfc.nasa.gov/>) for the NCME from 1997 to 2008. We used the CHL to construct the cumulative phytoplankton biomass as a function of cell size each year as described in Appendix C. The cumulative biomass was then partitioned to construct time series of the biomass of three primary size groups: $\tilde{B}_i(t)$, where $i \in \{\text{pico, nano, micro}\}$. We identified the year 1998 as the least productive in terms of CHL and also as the warmest (it was an El Niño year) (Yáñez et al. 2008).

To obtain the plankton size spectrum for 1998, we calculated the scaling factor $\tilde{B}_{i,1998}/\tilde{B}_{i,2008}$ for each \tilde{B}_i . The numerical density $N_{i,1998}$ of each group i in 1998 was taken as $N_{i,2008} \times \tilde{B}_{i,1998}/\tilde{B}_{i,2008}$, where $N_{i,2008}$ is the numerical density of group i in the survey data of 2008 (cool year). With these numerical densities, a phytoplankton size spectrum was obtained for warm conditions. In keeping with size-spectrum theory, a linear projection from the largest phytoplankton through the zooplankton body sizes was assumed to obtain the full plankton spectrum for warm conditions for 1998. Using a linear regression analysis, the slope (λ_p) of plankton spectrum for warm conditions was estimated, and the density U_{p,x_0} was obtained at $x_0 = -23$ as in cool conditions (Table 1).

Feeding preference functions

Morphological studies on the feeding apparatus of anchovy and sardine in the Benguela system have shown structural dissimilarities between the species and developmental changes with body size. Anchovy has a larger gill-raker gap and gape than sardine,

Fig. 1. (a) A feeding kernel that retains its shape as predator body mass increases. (b) A planktivore feeding kernel in which a fish continues feeding on small plankton particles as it grows.



indicating that it consumes larger prey than sardine (van der Lingen et al. 2006, 2009). In both species, gill arch and raker length increase as individuals grow, and additionally, the number of gill rakers increases with body size in sardine. Similar evidence has been found in two related species in the Bay of Biscay, the anchovy (*Engraulis encrasicolus*) having a greater gape width and height than the sardine (*Sardina pilchardus*), together with changes as body size increases (Bachiller and Irigoien 2013).

Although detailed morphological studies of feeding apparatus of the species are not available for the Humboldt Ecosystem, the evidence available is consistent with the data from Benguela and the Bay of Biscay. The species have different mouth sizes, with anchovy consuming larger prey than sardine; mouth width and prey size of sardine and anchovy larvae also increase linearly with body length (Muck et al. 1989). The studies of anchovy and sardine off the Northern Peruvian Ecosystem (Espinoza and Bertrand 2008; Espinoza et al. 2009) showed that sardine can feed on particles about 100 times smaller than anchovy, the smallest prey sizes being approximately $\exp(x'_{a,\min}) = 10^{-8}$ g for anchovy and $\exp(x'_{s,\min}) = 10^{-10}$ g for sardine. Carbon content of anchovy's prey moves increasingly from copepods to euphausiids, i.e., from smaller to larger prey items, as it grows (Espinoza and Bertrand 2014). In addition to developing a capacity to feed on larger particles (zooplankton) during growth, both species retain the ability to filter-feed on phytoplankton as they grow, thereby causing their diets to become broader (Espinoza and Bertrand 2008; Espinoza et al. 2009; Medina et al. 2015).

Previous models of size-spectrum dynamics have not allowed for diet broadening as body size increases. Typically, the distribution (feeding kernel) $\phi_i(x, x')$ of preferred food item sizes x' for an individual of species i at size x has been assumed to be log-normal (Ursin 1973), with a fixed mean (log of a preferred predator-prey mass ratio (PPMR) β_i) and a fixed diet breadth σ_i (Blanchard et al. 2009; Law et al. 2009; Andersen and Pedersen 2010; Hartvig et al. 2011). This shifts the feeding kernel towards larger prey as predators increase in size without changing its shape on the log mass scale. Figure 1 illustrates the assumption of a fixed feeding kernel in comparison with a planktivore that retains a capacity for filter-feeding on small plankton (phytoplankton) as it grows.

To allow diet breadth to increase, we modified the feeding kernel $\phi_i(x, x')$:

$$(1) \quad \phi_i(x, x') = \frac{1}{\sigma_i(x)\sqrt{2\pi}} \exp\left[-\frac{((x - x') - \beta_i(x))^2}{2\sigma_i(x)^2}\right]$$

making both $\beta_i(x)$ and $\sigma_i(x)$ functions of body size x :

$$(2) \quad \beta_i(x) = \frac{x - x'_{i,\min} + \log_e 10}{2}$$

$$(3) \quad \sigma_i(x) = \frac{\beta_i(x) - \log_e 10}{3}$$

with the function ϕ_i being truncated at 3 times σ_i and normalised to integrate to 1. This is a model with just one parameter ($x'_{i,\min}$) that allows a predator of size x to feed on prey from size $x'_{i,\min}$ up to $x - \log_e(10)$, i.e., up to 0.1 of the body mass of the predator, the preference function being symmetric and centered on the midpoint of that range.

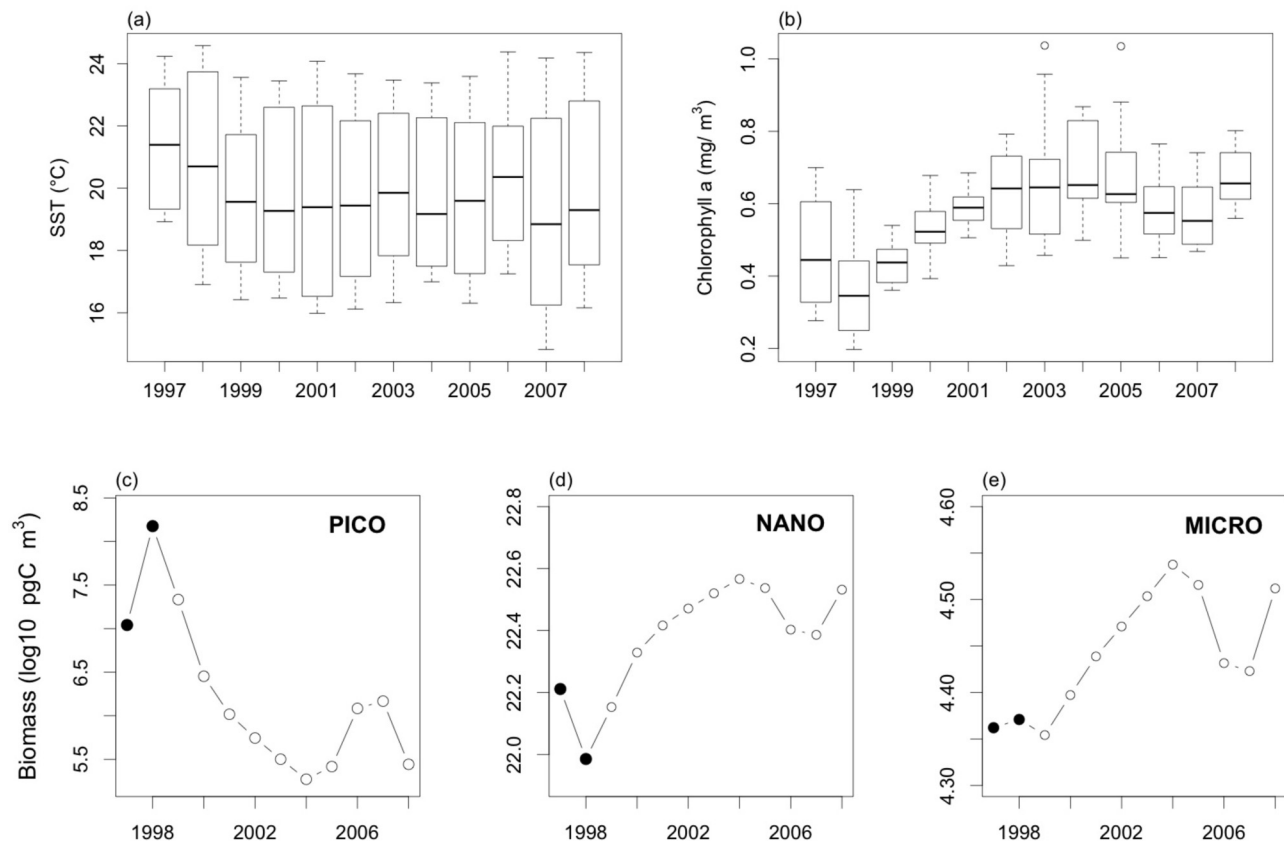
The specification of the feeding preference function was completed with a mass to set the level of feeding by anchovy and sardine on their own species (cannibalism) and on other taxa (interspecific predation and plankton). The mass was a dimensionless scalar θ_{ij} and independent of body size (Hartvig et al. 2011).

Predation simulation experiments

Numerical integrations were carried out to investigate the response of anchovy and sardine to fixed plankton size spectra representing different plankton size composition under cool and warm conditions. We ran the simulations for 100 years to generate strong signals of the effects of the contrasting plankton spectra and to identify the asymptotic states of the fish species. Clearly, the responses generated by an El Niño event in a single year would be a small fraction of these, but decadal oscillations on the time scale of anchovy-sardine fluctuations would be expected to generate changes near to those modelled. We recorded a species as collapsed if its total density was $\leq 10^{-4} \text{ m}^{-3}$ after 100 years. If the density was above this threshold and not varying over time, the species was recorded as being present and at equilibrium. If the density was oscillating, the species was recorded as having a nonequilibrium asymptotic state. An integration step size $dt = 0.0001$ was used, as well as a body-size step $dx = 0.1$, with initial conditions as given in Appendix B.

To examine the effects of cannibalism and predation, we included a parameter θ_{ij} in the feeding function to control the strength of cannibalism and interspecific predation. θ_{ij} had a range of 0 to 1, corresponding to the degree to which type i consumed prey of type j . The set of θ s can be thought of as analogous to an interaction matrix and could, for instance, be determined by the extent of spatial overlap (Blanchard et al. 2014). A value $\theta_{ij} = 0$ indicates no feeding of i on j , and a value of 1 indicates full feeding. For instance, if $\theta_{ij} = 1$ when $i = j$, and $\theta_{ij} = 0$ when $i \neq j$, then species i feeds on itself (cannibalism) but

Fig. 2. (a, b) Box-whisker plots of satellite sea surface temperature (SST, °C) and chlorophyll *a* (mg·m⁻³) at NCME from 1997 to 2008. Biomasses (log₁₀ pg C·m⁻³) predicted from yearly estimates of size spectra for (c) pico-, (d) nano-, and (e) micro-plankton. (Black dots indicate the warm event of 1997–1998.)



not on the other fish species. For simplicity, we kept a symmetry $\theta_{aa} = \theta_{ss}$ and $\theta_{as} = \theta_{sa}$ when varying the strength of cannibalism and intraspecific predation. Because anchovy and sardine are both planktivorous, we set $\theta_{ap} = \theta_{sp} = 1$ to allow full feeding on the plankton.

As well as feeding on plankton, anchovy and sardine are known to feed on their own species and also to experience interspecific predation. Anchovy cannibalism has been reported in California, Peru, and Benguela (Hunter and Kimbrell 1980; Alheit 1987; Valdés-Szeinfeld 1991) and off the coasts of Argentina and Portugal (Pájaro et al. 2007; Garrido et al. 2008). Cannibalism and IGP predation were estimated to account for 6% to 56%, respectively, of egg mortality in anchovy (Valdés-Szeinfeld 1991), and cannibalism in the Iberian sardine (*Sardina pilchardus*) accounted for 81% of the egg mortality (Garrido et al. 2008).

Results

Plankton

We identified 1997 and 2008 as the two contrasting years to approximate plankton size composition based on differences in sea surface temperatures (SSTs) in the NCME (Fig. 2a). In the years 1997 and 1998, the NCME was also under the influence of a strong El Niño event, creating unfavourable temporal conditions for anchovy (Yáñez et al. 2008). Overall, a shift from warm to mostly cool conditions was observed from 1999 onwards in the NCME.

During the period 1997 to 2008, NCME also experienced large changes in chlorophyll *a*, indicative of a change in the phytoplankton assemblage (Fig. 2b). Chlorophyll *a* was especially low in 1997 and 1998 and then increased for several years, with a small fall in 2006 and 2007. The change in the phytoplankton assemblage was clear when its size spectrum was partitioned into size

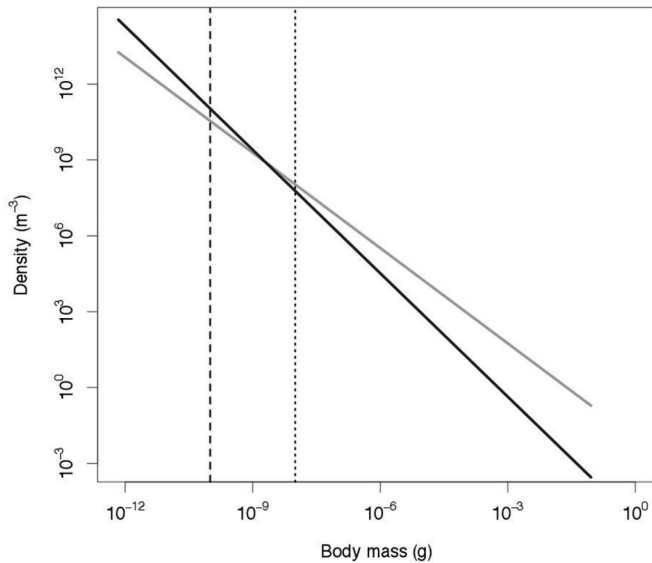
groups. Picoplankton was at its greatest biomass density in 1998, after which it fell to lower values (Fig. 2c). Nano- and microplankton showed the opposite trend (Figs. 2d, 2e). In other words, phytoplankton biomass was more concentrated at the smallest cell sizes under warm conditions and more spread out over cell size in the cool conditions.

The plankton spectrum for 1998 had a slope of -1.63 , steeper and outside the confidence interval of the plankton spectrum fitted to the 2008 survey data obtained under more cool conditions (-1.26 ; 95% CI -1.37 to -1.14) (Fig. 3). The two plankton spectra intersect at a body mass of 10^{-9} g. This means that body sizes less than 10^{-9} g have greater densities under warm conditions than under cool conditions, and body sizes greater than 10^{-9} g have lower densities (Fig. 3). We used these two plankton spectra in the simulations of the fish size spectra that follow as representative of cool and warm conditions.

Fish feeding on plankton without cannibalism or interspecific predation

The PPMR of sardine extends to greater values than that of anchovy (Figs. 4a, 4b); for instance, for a predator of body mass of 10 g, the maximum $\log_e(\text{PPMR})$ is approximately 20 in anchovy and 25 in sardine. Put another way, sardine feeds further down into the plankton than anchovy, as shown in Fig. 3. Feeding just on the plankton, both species could persist (at equilibrium) under smaller (warm) and larger (cool) plankton size conditions. At this equilibrium, the total consumption rates of both species were reduced in warm conditions, but sardine maintained a higher consumption rate than anchovy by virtue of its feeding apparatus (Figs. 4c, 4d). Both species grew more slowly in body size under smaller plankton conditions (Figs. 4e, 4f) because of their lower

Fig. 3. Predicted size structure of the plankton community in warm conditions (1998, black) and cool conditions (2008, grey). Dash and dotted lines indicate the lower limit of the feeding kernel of sardine (10^{-10} g) and anchovy (10^{-8} g), respectively.



consumption rates, but anchovy suffered more, being less able to feed low in the plankton spectrum.

Fish feeding on plankton with cannibalism and interspecific predation

Figure 5 shows the long-term outcome in our simulations when planktivory under small (warm) and large (cool) plankton availability was combined with a range of cannibalism and interspecific predation. Anchovy and sardine coexisted when larger plankton (cool) were available (Figs. 5a, 5b) over a wide range of cannibalism and interspecific predation (low cannibalism and strong interspecific predation led to the collapse of sardine). However, under a shift towards smaller plankton (typical of warmer conditions), anchovy collapsed over a wide range of predation pressures, whereas sardine did not (Figs. 5c, 5d).

Over most of the parameter ranges tested, both species went to an equilibrium state. However, there were exceptions. In large-sized plankton conditions, strong cannibalism combined with weak interspecific predation led to oscillations in both species (Figs. 5a, 5b). An oscillatory state also came about under the same plankton conditions when an intermediate level of cannibalism was combined with strong interspecific predation. This was apparently driven by an interspecific predator-prey cycle of abundant large anchovy eating small sardine (results not shown). In smaller plankton conditions, anchovy developed oscillations under strong cannibalism and weak interspecific predation. However, anchovy's density was low enough and interspecific predation was weak enough for there to be no detectable effect of these oscillations on the sardine population (Figs. 5c, 5d).

Discussion

We show that differences in the plankton size spectrum can have major consequences for the growth and coexistence of sardine and anchovy using simplified equilibrium scenarios from a dynamical multispecies size-spectrum model. How these effects combine with multiple dynamic oceanographic and ecosystem processes influencing sardine-anchovy fluctuations would require further study. However, our results provide evidence that the phytoplankton size spectrum in NCME was steeper in warm than in cool conditions during the period 1997 to 2008. The density of picoplankton was greater, and microplankton was lower,

when conditions were warm. These results are also consistent with a general tendency for picoplankton to be more abundant in warmer seas (Agawin et al. 2000; Iriarte and González 2004; Morán et al. 2010) and the steeper slopes of the phytoplankton spectrum in warm aquatic ecosystems (Yvon-Durocher et al. 2011).

Extending the plankton spectrum from the phytoplankton to larger body sizes leads to the expectation that zooplankton densities would be reduced in warm conditions. Several studies reported shifts towards smaller body size in the zooplankton in the NCME during warm conditions. These include a decrease in the abundance of copepods in the coastal waters off Mejillones (Hidalgo and Escribano 2001), a gradual decrease of large zooplankton such as euphausiids in the areas off northern Chile (González et al. 2000), and a shift in size structure of *Calanus chilensis* (copepod) towards smaller body size (Ulloa et al. 2001).

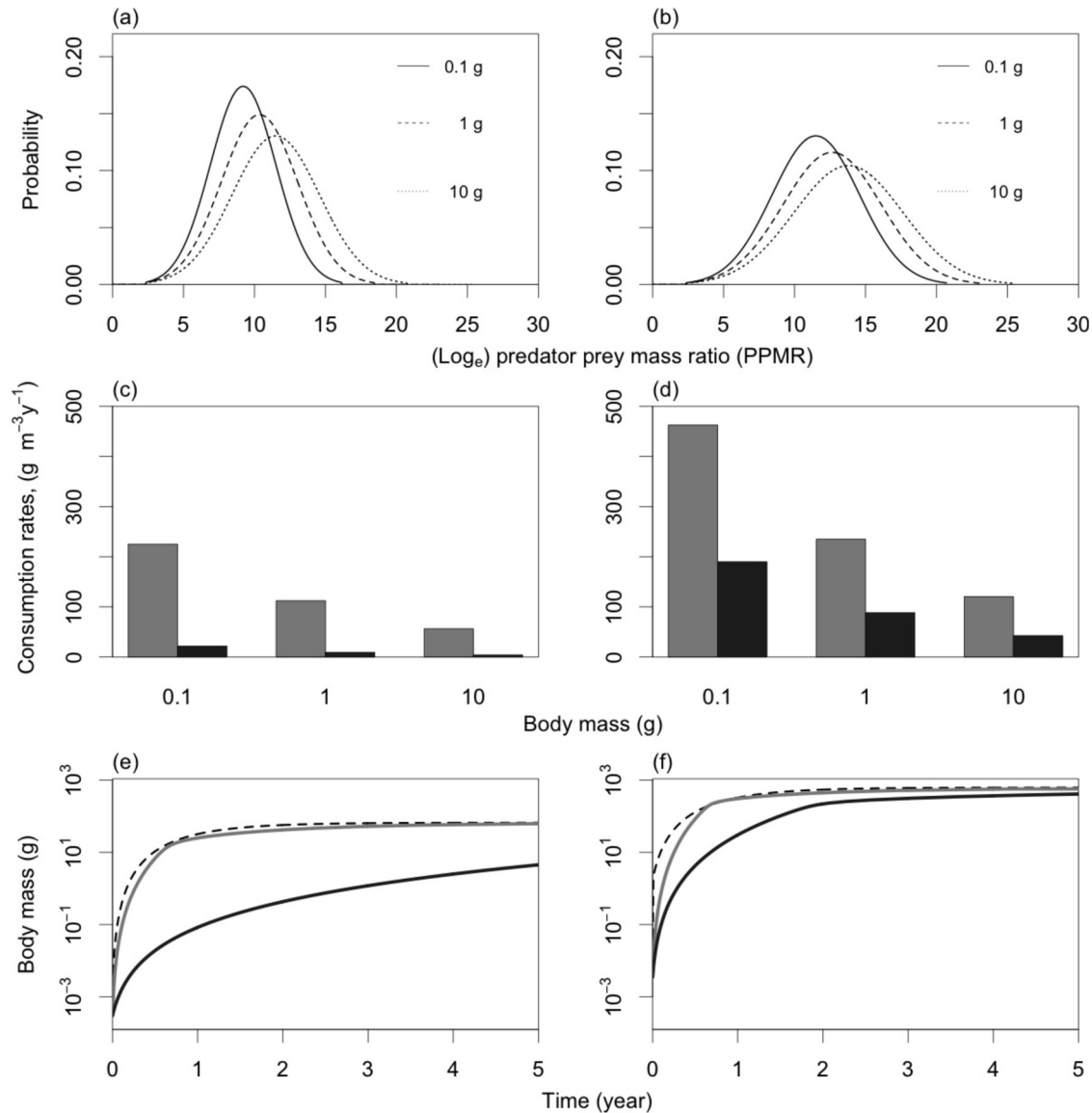
Numerical results from our size-spectrum model suggest that the change in the plankton spectrum has effects that percolate through the pelagic food web due to differences in the feeding apparatus of the two main planktivores, anchovy and sardine (van der Lingen et al. 2006, 2009). The feeding morphology of sardine allows it to extract particles with masses smaller than anchovy and, therefore, to feed more on the small plankton. Consistent with this, Ayón et al. (2011), for instance, found that the temporal pattern for euphausiid dominance was highly cross-correlated (in phase) with anchovy biomass and small zooplankton dominance with sardine biomass in the Northern Humboldt Ecosystem over the period 1963 to 2005. The direct effect of the switch to a steeper spectrum in our analysis was to reduce the growth rate of individuals of both species, substantially more so in anchovy than in sardine, thereby increasing anchovy's vulnerability to predation disproportionately. This change in individual growth of both species is a prediction that could readily be tested using otoliths to reconstruct biochronologies (Morrongiello et al. 2012).

As the planktivores grow, they become predators on smaller individuals of both species, while still filter-feeding down the plankton spectrum (Valdés-Szeinfeld 1991; Alheit 1987; Medina et al. 2015). Modifying the feeding kernels of standard size-spectrum models to incorporate this behavior amplified the effects of the changes in the plankton spectra, anchovy being unable to persist at high density with sardine in small plankton (warm) conditions under most combinations of cannibalism and predation in our simulations. In large plankton (cool) conditions, sardine was able to persist with anchovy unless cannibalism was small and interspecific predation was large. These results support the suggestion that there are synergies caused by cannibalism and predation among the planktivores (Valdés-Szeinfeld 1991) and that IGP could be an important process in the dynamics of these fish population (Irigoien and de Roos 2011).

These results are consistent with the food web effect suggested by Alheit and Niquen (2004) and MacCall (2009) that changes in the oceanographic conditions (here, temperature), whether oscillatory or permanent, set in motion a number of changes in the trophic relations of anchovy and sardine both as predators and prey favoring sardine in warmer and anchovy in cooler conditions. Thus, fluctuations in temperature in the ecosystem may affect these populations in multiple ways: distribution (Bertrand et al. 2004, 2011), larval growth (Takasuka et al. 2007), and in the growth-predation system as shown here.

From another perspective, SST clearly has other indirect effects on marine ecosystems in addition to its effect on the shape of plankton spectra. For instance, increasing temperature reduces the solubility of oxygen and increases the demand for oxygen, reducing the maximum size to which fish grow. As a result, future climates are predicted to bring a substantial fall in the global mass of fish (Cheung et al. 2013), a prediction supported by empirical results in the North Sea (Baudron et al. 2014). Even without explicitly considering the effects of temperature on growth, such effects

Fig. 4. Anchovy (left) and sardine (right) in small (dark grey) and large (light grey) plankton conditions. (a, b) Feeding preference functions at three predator sizes (0.1, 1, and 10 g). (c, d) Consumption rates at the same predator sizes, computed at steady state. (e, f) Growth trajectories from feeding on plankton at steady state for anchovy and sardine. For comparison, von Bertalanffy growth equations from literature (black dashed lines) are included (Appendix B, Table B1).

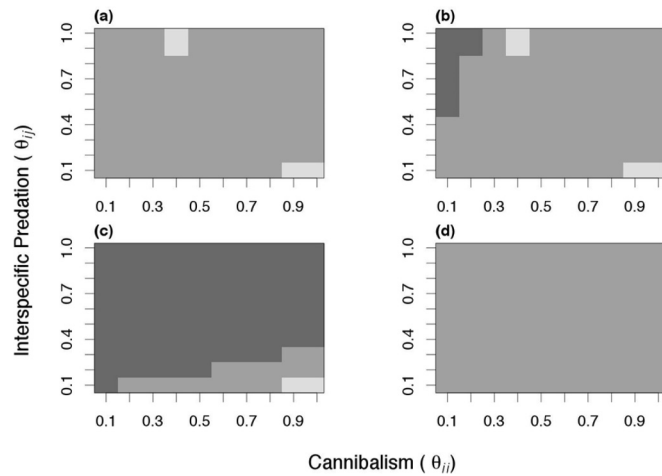


of climate change can be linked to growth via changes in planktonic size structure (Woodworth-Jefcoats et al. 2012). Our results suggest the reductions in fish growth, as plankton spectra become tilted towards the picoplankton, can be accompanied by substantial restructuring of the fish assemblage. These climate-induced impacts on phytoplankton size structure can propagate all the way through the marine size spectrum ultimately affecting fisheries catches (Woodworth-Jefcoats et al. 2012; Barange et al. 2014). Further work on the joint effects of environmental drivers and the size structure of food on fish growth in a community context is clearly needed to assess model uncertainty associated with this and other studies (Brander et al. 2013).

Size-spectrum models do the bookkeeping of biomass in more detail than marine ecosystem models have previously done (Law et al. 2014) but necessarily still simplify very complex systems (Fulton et al. 2011). To ensure that the plankton spectra corresponded to those observed in cool and warm conditions, we held the plankton spectra fixed under cool and warm conditions and did not incorporate the complex dynamics of the plankton com-

munity. In reality, anchovy and sardine are embedded in more complicated ecosystems, and it remains to be seen how other predators and fishing affect the anchovy-sardine fluctuations. In the absence of detailed information about the feeding kernels of the anchovy and sardine, we made simple assumptions about their shape, consistent with their feeding apparatus and data available on their diets. We made a direct link between the climate variability (SST) and the pelagic system of NCME through changes in the size structure of the phytoplankton community contrasting cool and warm conditions. We detected a change in the slope of the plankton and in the intercept; however, we think that the last one could change more dramatically than described here. The most direct way of making this link would be through direct measurement of plankton size spectrum under different environmental conditions, but this was not available. Nonetheless, uncertainty about the exact change, particularly in the intercept of the phytoplankton spectrum during cool to warm conditions, still exists and needs to be validated with observational data. In keeping with most other size-spectrum models, we assumed that dynam-

Fig. 5. Combined effects of feeding on plankton, interspecific predation, and cannibalism: (a, c) anchovy; (b, d) sardine; (a, b) large plankton (cool); (c, d) small plankton (warm). Shading indicates the state of the numerical density at the end of the simulation period: medium gray = species present and at equilibrium; light gray = species present and oscillating; dark gray = species collapsed.



ics took place in a homogeneous space. In reality, physical processes in the HCS modify the three-dimensional distribution of physical (e.g., temperature), chemical (e.g., oxygen), and biological (e.g., plankton) parameters, and mobile fish are likely to respond to this spatial variation in different ways (Bertrand et al. 2008). For instance, Bertrand et al. (2004) proposed that during the El Niño of 1997–1998, anchovy was able to exploit small-scale temporal and spatial “loop-holes”, i.e., refugia, in an otherwise unfavourable environment. Refugia would not prevent a large decrease in abundance of anchovy, because such places would be small compared with those in which anchovy would live under cooler conditions. However, refugia would help to retain a residual population of anchovy and allow faster recovery when conditions improved.

Overall, we suggest that the oceanographic conditions in the HCS (Alheit and Niquen 2004; Bertrand et al. 2004; Yáñez et al. 2008) associated with long-term warm conditions, a deeper thermocline, and a weak upwelling could trigger the following effects in the pelagic food web of the NCME: (1) low biomass and productivity of the phytoplankton community and a shift towards smaller body size in the zooplankton community; (2) reduced growth rates of both fish species shifting them towards smaller body sizes; and (3) a more deleterious effect on anchovy because it is unable to feed on smaller plankton. The cumulative result would be to make both species more vulnerable to predation, the effects being more deleterious on anchovy than on sardine. These predictions have implications for fishing and climate change, they are open to empirical tests, and they may apply to other upwelling systems.

Acknowledgements

T.M. Canales acknowledges the National Commission for Scientific and Technological Research (CONICYT) – Chile and the Holbeck Foundation (UK) for funding her Ph.D. studies. T.M. Canales is now funded by the project CONICYT-PIA FB 0002 (2014). We are grateful for the helpful comments of two anonymous reviewers of this paper. We thank the Fisheries Research Fund (FIP) – Chile and Mauricio Braun for supplying the plankton data for this paper.

References

Agawin, N.S.R., Duarte, C.M., and Agustí, S. 2000. Nutrient and temperature control of the contribution of picoplankton to phytoplankton biomass and production. *Limnol. Oceanogr.* 45(3): 591–600. doi:10.4319/lo.2000.45.3.0591.

Alheit, J. 1987. Egg cannibalism versus egg predation: their significance in anchovies. *South Afr. J. Mar. Sci.* 5: 467–470. doi:10.2989/025776187784522694.

Alheit, J., and Niquen, M. 2004. Regime shifts in the Humboldt Current ecosystem. *Prog. Oceanogr.* 60: 201–222. doi:10.1016/j.poccean.2004.02.006.

Andersen, K.H., and Beyer, J.E. 2006. Asymptotic size determines species abundance in the marine size spectrum. *Am. Nat.* 168: 54–61. doi:10.1086/504849.

Andersen, K.H., and Pedersen, M. 2010. Damped trophic cascades driven by fishing in model marine ecosystems. *Proc. R. Soc. B Biol. Sci.* 277: 795–802. doi:10.1098/rspb.2009.1512.

Ayón, P., Swartzman, G., Espinoza, P., and Bertrand, A. 2011. Long-term changes in zooplankton size distribution in the Peruvian Humboldt Current System: conditions favouring sardine or anchovy. *Mar. Ecol. Prog. Ser.* 422: 211–222. doi:10.3354/meps08918.

Bachiller, E., and Irigoien, X. 2013. Allometric relations and consequences for feeding in small pelagic fish in the Bay of Biscay. *ICES J. Mar. Sci.* 70: 232–243. doi:10.1093/icesjms/fss171.

Bakun, A. 2001. “School-mix feedback”: a different way to think about low frequency variability in large mobile fish populations. *Prog. Oceanogr.* 49: 485–511. doi:10.1016/S0079-6611(01)00037-4.

Bakun, A., and Cury, P. 1999. The “school trap”: a mechanism promoting large-amplitude out-of-phase population oscillations of small pelagic fish species. *Ecol. Lett.* 2: 349–351. doi:10.1046/j.1461-0248.1999.00099.x.

Barange, M., Merino, G., Blanchard, J.L., Scholtens, J., Allison, E.H., Allen, J.I., Holt, J., and Jennings, S. 2014. Impacts of climate change on marine ecosystem production in societies dependent on fisheries. *Nat. Clim. Change*, 4(3): 211–216. doi:10.1038/nclimate2119.

Barnes, C., Irigoien, X., de Oliveira, J., Maxwell, D., and Jennings, S. 2011. Predicting marine phytoplankton community size structure from empirical relationships with remotely sensed variables. *J. Plankt. Res.* 33: 13–24. doi:10.1093/plankt/fbq088.

Baudron, A.R., Needle, C.L., Rijnsdorp, A.D., and Marshall, C.T. 2014. Warming temperatures and smaller body sizes: synchronous changes in growth of North Sea fishes. *Glob. Change Biol.* 20(4): 1023–1031. doi:10.1111/gcb.12514.

Bertrand, A., Segura, M., Gutiérrez, M., and Vásquez, L. 2004. From small-scale habitat loop-holes to decadal cycles: a habitat-based hypothesis explaining fluctuation in pelagic fish populations off Peru. *Fish Fish.* 5: 296–316. doi:10.1111/j.1467-2679.2004.00165.x.

Bertrand, A., Chaigneau, A., Peraltila, S., Ledesma, J., Graco, M., Monetti, F., and Chavez, F.P. 2011. Oxygen: a fundamental property regulating pelagic ecosystem structure in the coastal southeastern tropical Pacific. *PLoS ONE*, 6: 1–8. doi:10.1371/journal.pone.0029558.

Bertrand, S., Díaz, E., and Lengaigne, M. 2008. Patterns in the spatial distribution of Peruvian anchovy (*Engraulis ringens*) revealed by spatially explicit fishing data. *Prog. Oceanogr.* 79: 379–389. doi:10.1016/j.poccean.2008.10.009.

Blanchard, J.L., Jennings, S., Law, R., Castle, M.D., McCloghrie, P., Rochet, M.-J., and Benoit, E. 2009. How does abundance scale with body size in coupled size-structured food webs? *J. Anim. Ecol.* 78: 270–280. doi:10.1111/j.1365-2656.2008.01466.x.

Blanchard, J.L., Andersen, K.H., Scott, F., Hintzen, N.T., Piet, G., and Jennings, S. 2014. Evaluating targets and trade-offs among fisheries and conservation objectives using a multispecies size spectrum model. *J. Appl. Ecol.* 51(3): 612–622. doi:10.1111/1365-2664.12238.

Brander, K., Neuheimer, A., Andersen, K.H., and Hartvig, M. 2013. Overconfidence in model projections. *ICES J. Mar. Sci.* 70: 1065–1068. doi:10.1093/icesjms/fst055.

Braun, M., Reyes, H., Pizarro, E.M., Herrera, L., Santander, E., Claramunt, G., Oliva, E., Valenzuela, V., Catasti, V., Saavedra, J., et al. 2009. Monitoreo de las condiciones bio-oceanográficas entre la I y IV Regiones, año 2008. Fondo de Investigación Pesquera, Informe Final FIP/2008-21; www.fip.cl.

Canales, T.M., and Leal, E. 2009. Life history parameters of anchoveta, *Engraulis ringens* Jenyns, 1842, in central north Chile. *Rev. Biol. Mar. Oceanogr.* 44: 173–179. doi:10.4067/S0718-19572009000100017.

Chavez, F.P., Ryan, J., and Lluch-Cota, S.E., and Niquen, M. 2003. From anchovies to sardines and back: multidecadal change in the Pacific Ocean. *Science*, 299: 217–221. doi:10.1126/science.1075880.

Cheung, W.W.L., Sarmiento, J.L., Dunne, J., Frölicher, T.L., Lam, V.W.Y., Palomares, M.L.D., Watson, R., and Pauly, D. 2013. Shrinking of fishes exacerbates impacts of global ocean changes on marine ecosystems. *Nat. Clim. Change*, 3: 254–258. doi:10.1038/NCLIMATE1691.

Cury, P. 1994. Obstinate nature: an ecology of individuals. Thoughts on reproductive behavior and biodiversity. *Can. J. Fish. Aquat. Sci.* 51(7): 1664–1673. doi:10.1139/f94-167.

Espinoza, P., and Bertrand, A. 2008. Revisiting Peruvian anchovy (*Engraulis ringens*) trophodynamics provides a new vision of the Humboldt Current system. *Prog. Oceanogr.* 79: 215–227. doi:10.1016/j.poccean.2008.10.022.

Espinoza, P., and Bertrand, A. 2014. Ontogenetic and spatiotemporal variability in anchoveta *Engraulis ringens* diet off Peru. *J. Fish Biol.* 84: 422–435. doi:10.1111/jfb.12293.

Espinoza, P., Bertrand, A., van der Lingen, C.D., Garrido, S., and Rojas de Mendiola, B. 2009. Diet of sardine (*Sardinops sagax*) in the northern Humboldt Current system and comparison with the diets of clupeoids in this and other eastern boundary upwelling systems. *Prog. Oceanogr.* 83: 242–250. doi:10.1016/j.poccean.2009.07.045.

Essington, T., Moriarty, P.E., Froehlich, H.E., Hodgson, E.E., Koehn, L.E., Oken, K.L., Siple, M.C., and Stawitz, C.C. 2015. Fishing amplifies forage fish

- population collapses. *Proc. Natl. Acad. Sci.* **112**(21): 6648–6652. doi:10.1073/pnas.1422020112.
- Fréon, P., Barange, M., and Aristegui, J. 2009. Eastern Boundary Upwelling Ecosystems: integrative and comparative approaches. *Prog. Oceanogr.* **83**: 1–14. doi:10.1016/j.pocean.2009.08.001.
- Fulton, E.A., Link, J.S., Kaplan, I.C., Savina-Rolland, M., Johnson, P., Ainsworth, C., Horne, P., Gorton, R., Gamble, R.J., and Smith, A.D.M. 2011. Lessons in modelling and management of marine ecosystems: the Atlantis experience. *Fish. Fish.* **12**: 171–188. doi:10.1111/j.1467-2979.2011.00412.x.
- Garrido, S., Ben-Hamadou, R., Oliveira, P., Cunha, M., Chicharo, M., and van der Lingen, C. 2008. Diet and feeding intensity of sardine *Sardina pilchardus*: correlation with satellite-derived chlorophyll data. *Mar. Ecol. Prog. Ser.* **354**: 245–256. doi:10.3354/meps07201.
- González, H.E., Sobarzo, M., Figueroa, D., and Nöthing, E-M. 2000. Composition, biomass and potential grazing impact of the crustacean and pelagic tunicates in the northern Humboldt Current area off Chile: differences between El Niño and non-El Niño years. *Mar. Ecol. Prog. Ser.* **195**: 201–220. doi:10.3354/meps195201.
- Hartvig, M., and Andersen, K.H. 2013. Coexistence of structured populations with size-based prey selection. *Theor. Popul. Biol.* **89**: 24–33. doi:10.1016/j.tpb.2013.07.003.
- Hartvig, M., Andersen, K.H., and Beyer, J.E. 2011. Food web framework for size-structured populations. *Theor. Popul. Biol.* **77**: 113–122. doi:10.1016/j.tpb.2010.12.006.
- Hidalgo, P., and Escribano, R. 2001. Succession of pelagic copepod species in coastal waters off northern Chile: the influence of the 1997–98 El Niño. *Hydrobiologia*, **453/454**: 153–160. doi:10.1023/A:1013188522222.
- Hunter, J.R., and Kimbrell, C.M. 1980. Egg cannibalism in the Northern Anchovy, *Engraulis mordax*. *Fish. Bull.* **78**: 811–816.
- Iriarte, J., and González, H. 2004. Phytoplankton size structure during and after the 1997/98 El Niño in a coastal upwelling area of the northern Humboldt Current System. *Mar. Ecol. Prog. Ser.* **269**: 83–90. doi:10.3354/meps269083.
- Irigoin, X., and de Roos, A. 2011. The role of intraguild predation in the population dynamics of small pelagic fish. *Mar. Biol.* **158**: 1683–1690. doi:10.1007/s00227-011-1699-2.
- Law, R., Plank, M.J., James, A., and Blanchard, J.L. 2009. Size-spectra dynamics from stochastic predation and growth of individuals. *Ecology*, **90**: 802–811. doi:10.1890/07-1900.1.
- Law, R., Plank, M.J., and Kolding, J. 2014. Balanced exploitation and coexistence of interacting, size-structured fish species. *Fish. Fish.* doi:10.1111/faf.12098.
- Lluch-Belda, D., Crawford, R.J.M., Kawasaki, T., MacCall, A.D., Parrish, R.H., Schwartzlose, R.A., and Smith, P.E. 1989. World-wide fluctuations of sardine and anchovy stocks: the regime problem. *South African J. Mar. Sci.* **8**: 195–205. doi:10.2989/02577618909504561.
- MacCall, A.D. 2002. An hypothesis explaining biological regimes in sardine-producing Pacific Boundary Current Systems (South America, North America and Japan): implications of alternating modes of slow, meandering flow and fast, linear flow in the offshore region. In *Climate and fisheries. Interacting paradigms, scales, and policy approaches.* Edited by A. Bakun and K. Broad. International Research Institute for Climate Prediction, Columbia University. pp. 39–42.
- MacCall, A.D. 2009. Mechanism of low-frequency fluctuations in sardine and anchovy populations. In *Climate change and small pelagic fish.* Edited by D. Checkley. Cambridge University Press.
- McKendrick, A.G. 1925. Applications of mathematics to medical problems. *Proc. Edinb. Math. Soc.* **44**: 98–130. doi:10.1017/S0013091500034428.
- Medina, M., Herrera, L., Castillo, J., Jaque, J., and Pizarro, N. 2015. Alimentación de la anchoveta (*Engraulis ringens*) en el norte de Chile (18°25'–25°40'S) en diciembre de 2010. *Lat. Am. J. Aquat. Res.* **43**(1): 46–58. doi:10.3856/vol43-issue1-fulltext-5.
- Morán, X.A.G., López-Urrutia, A., Calvo-Díaz, A., and Li, W.K.W. 2010. Increasing importance of small phytoplankton in a warmer ocean. *Glob. Change Biol.* **16**: 1137–1144. doi:10.1111/j.1365-2486.2009.01960.x.
- Morrongiello, J.R., Thresher, R.E., and Smith, D.C. 2012. Aquatic biochronologies and climate change. *Nat. Clim. Change*, **2**: 849–857. doi:10.1038/NCLIMATE1616.
- Muck, P., Rojas de Mendiola, B., and Antonietti, E. 1989. Comparative studies on feeding in larval anchoveta (*Engraulis ringens*) and sardine (*Sardinops sagax*). In *The Peruvian upwelling ecosystem: dynamics and interactions.* Edited by D. Pauly, P. Muck, J. Mendo, and I. Tsukayama. ICLARM Conference Proceedings, Vol. 18. pp. 86–96.
- Pájaro, M., Curelovich, J., and Macchi, G.J. 2007. Egg cannibalism in the northern population of the Argentine anchovy, *Engraulis anchoita* (Clupeidae). *Fish. Res.* **83**: 253–262. doi:10.1016/j.fishres.2006.09.014.
- Rijnsdorp, A.D., Peck, M.A., Engelhard, G.H., Möllmann, C., and Pinnegar, J.K. 2009. Resolving the effect of climate change on fish populations. *ICES J. Mar. Sci.* **66**: 1570–1583. doi:10.1093/icesjms/fsp056.
- Schwartzlose, R.A., Alheit, J., Bakun, A., Baumgartner, T.R., Cloete, R., Crawford, R.J.M., Fletcher, W.J., Green-Ruiz, Y., Hagen, E., Kawasaki, R., Lluch-Belda, D., Lluch-Cota, S., MacCall, A.D., Matsuura, Y., Nevarez-Martínez, M., Parrish, R.H., Roy, C., Serra, R., Shust, K., Ward, M.N., and Zuzugana, J.Z. 1999. Worldwide large-scale fluctuations of sardine and anchovy populations. *South Afr. J. Mar. Sci.* **21**: 289–347. doi:10.2989/025776199784125962.
- Sheldon, R.W., Prakash, A., and Sutcliffe, W.H., Jr. 1972. The size distribution of particles in the ocean. *Limnol. Oceanogr.* **17**: 327–340. doi:10.4319/lo.1972.17.3.0327.
- Takasuka, A., Oozeki, Y., and Aoki, I. 2007. Optimal growth temperature hypothesis: why do anchovy flourish and sardine collapse or vice versa under the same ocean regime?. *Can. J. Fish. Aquat. Sci.* **64**(5): 768–776. doi:10.1139/f07-052.
- Ulloa, O., Escribano, R., Hormazabal, S., Quiñones, R., González, R., and Ramos, M. 2001. Evolution and biological effects of the 1997–98 El Niño in the upwelling ecosystem off northern Chile. *Geophys. Res. Lett.* **28**: 1591–1594. doi:10.1029/2000GL011548.
- Ursin, E. 1973. On the prey size preferences of cod and dab. *Medd Dan Fisk Havunders.* **7**: 85–98.
- Valdés-Szeinfeld, E. 1991. Cannibalism and intraguild predation in clupeoids. *Mar. Ecol. Prog. Ser.* **79**: 17–26. doi:10.3354/meps079017.
- van der Lingen, C.D., Hutchings, L., and Field, J.G. 2006. Comparative trophodynamics of anchovy *Engraulis encrasicolus* and sardine *Sardinops sagax* in the southern Benguela: are species alternations between small pelagic fish trophodynamically mediated? *African J. Mar. Sci.* **28**: 465–477. doi:10.2989/18142320609504199.
- van der Lingen, C.D., Bertrand, A., Bode, A., Brodeur, R., Cubillos, L., Espinoza, P., Friedland, K., Garrido, S., Irigoien, X., Miller, T., Möllman, C., Rodríguez-Sánchez, R., Tanaka, H., and Temming, A. 2009. Trophic dynamics. In *Climate change and small pelagic fish.* Edited by D. Checkley. Cambridge University Press. 351 pp.
- Woodworth-Jefcoats, P.A., Polovina, J., Dunne, J.P., and Blanchard, J.L. 2012. Ecosystem size structure response to 21st century climate projection: large fish abundance decreases in the central North Pacific and increases in the California Current. *Glob. Change Biol.* **19**(3): 724–733. doi:10.1111/gcb.12076.
- Yáñez, E., Hormazabal, S., Silva, C., Montecinos, A., Barbieri, M.A., Valdenegro, A., Órdenes, A., and Gómez, F. 2008. Coupling between the environment and the pelagic resources exploited off northern Chile: ecosystem indicators and a conceptual model [Acomplamiento entre el ambiente y los recursos pelágicos explotados en el norte de Chile: un modelo conceptual]. *Lat. Am. J. Aquat. Res.* **36**: 159–181. doi:10.3856/vol36-issue-2-fulltext-3.
- Yvon-Durocher, G., Montoya, J.M., Trimmer, M., and Woodward, G. 2011. Warming alters the size spectrum and shifts the distribution of biomass in freshwater ecosystems. *Global Change Biol.* **17**(4): 1681–1694. doi:10.1111/j.1365-2486.2010.02321.x.

Appendix A. Model for size-spectrum dynamics

The size spectra of anchovy and sardine were dynamic, changing over time, through birth, growth, and death of individuals. The plankton spectrum was fixed in one of two alternative states so that the dynamics of the fish community under contrasting cool and warm conditions could be analyzed.

The state variables of the ecosystem were $N_a(w, t)$, $N_s(w, t)$, the density at time t of anchovy and sardine at body mass w per unit mass per unit volume (here $g^{-1}m^{-3}$). We used the log transformation $w = w_0 \exp(x)$ and density function $U_i(x, t) dx = N_i(w, t) dw$, with dynamics given by the McKendrick – von Foerster equation (Andersen and Beyer 2006; Hartvig et al. 2011; Hartvig and Andersen 2013; Blanchard et al. 2014), here taking the form

$$(A1) \quad \frac{\partial U_i}{\partial t} = \underbrace{-E_i \frac{\partial (g_i U_i)}{\partial x}}_{\text{(somatic growth)}} - \underbrace{(d_i + \mu_i) U_i}_{\text{(death)}} + \underbrace{\frac{b_i R_i}{w_0 e^x} D_i}_{\text{(reproduction)}}$$

where $i = a, s$. Most terms in this equation are functions, and their arguments have been omitted for clarity. The term $g_i(x, t)$ ($year^{-1}$) is the mass-specific rate at which biomass is assimilated by an individual of species i at size x and time t ; of this, a dimensionless proportion $E_i(x, t)$ is allocated to somatic growth and the remainder, $1 - E_i(x, t)$, goes to reproduction. Growth was achieved by eating other organisms and was therefore balanced by a per capita predation death rate $d_i(x, t)$ ($year^{-1}$). In addition, some death from other causes would be expected; this was given by a per capita rate $\mu_i(x, t)$ ($year^{-1}$). The term $R_i(t)$ is the total rate at which reproductive mass is generated in species i at time t ($g \cdot m^{-3} \cdot year^{-1}$). This mass rate was distributed over a birth kernel $b_i(x)$ normalised to sum to 1, assumed here to be a Dirac- δ function corresponding to the egg size $x_{i,egg}$ of species i . In this way, the total mass was divided into

packets of mass $w_0 \exp(x_{i,egg})$ to get the total rate at which eggs appeared. The term $D_i(x, t)$ made the egg production density dependent. Details on the functions are given below.

Bookkeeping of biomass as it passes from prey to predator formed the core of the model, with the consumption rate (year⁻¹) by a predator of type i ($i \in \{a, s\}$) and size x of prey of type j ($j \in \{p, a, s\}$) at size x' being given by the expression

$$(A2) \quad T_{ij}(x, x', t) = A e^{\alpha x} \phi_i(x, x') \theta_{ij} U_j(x', t)$$

This contains the volume searched by a predator per unit time as an allometric function of the body mass $A e^{\alpha x}$ (Ware 1978), where α is the allometric exponent and A is a parameter describing the volume searched per unit time per unit size (raised to the power α) (here: m³.year⁻¹.g^{- α}). The expression also contains a dimensionless feeding preference function $\phi_i(x, x')$; this differs from previous size-spectrum models to match the observed spreading of feeding (log-scaled) as planktivores increase in size (Fig. 1; eq. 1). The expression also contains the dimensionless scalar θ_{ij} , which determines the extent to which predators of type i consume prey of type j , and the density $U_j(x', t)$ of prey of type j at size x' at time t .

The mass-specific biomass assimilation rate $g_i(x, t)$ was obtained from eq. A2 by multiplying by prey mass, integrating over prey sizes x' and summing over prey types j to get the total rate of biomass consumption. Then, allowing for food conversion efficiency K and dividing by predator body mass, the mass-specific assimilation rate (year⁻¹) is

$$(A3) \quad g_i(x, t) = K A e^{(\alpha-1)x} \sum_j \theta_{ij} \int e^{x'} \phi_i(x, x') U_j(x', t) dx'$$

This is the rate before partitioning between somatic growth and reproduction.

The proportion of incoming biomass allocated to reproduction, $1 - E_i(x, t)$, went from 0 before maturation to a value 1 at an asymptotic body size $x_{i,\infty}$, the size at which all incoming mass went to reproduction. The function followed previous studies (Hartvig et al. 2011; Law et al. 2012) using the product of two factors:

$$(A4) \quad 1 - E_i(x) = \left[1 + \exp(\varepsilon_{i,0} - \varepsilon_{i,1}) \left(\frac{e^x}{a_i} \right)^{\frac{1}{b_i}} \right]^{-1} e^{\rho(x-x_{i,\infty})}$$

The first factor (in square brackets) corresponds to the maturity ogive, the proportion of individuals at size x that have reached maturity. Parameters $\varepsilon_{i,0}$ and $\varepsilon_{i,1}$ describe the maturity based on the body length, and parameters a_i and b_i transform the length into mass using the allometric relationship. The second factor (after the square brackets) describes the allocation to reproduction in a mature individual. We used an exponentially increasing function of size, reaching 1 at an asymptotic size $x_{i,\infty}$, with a scaling parameter ρ (Law et al. 2012).

The total rate of producing reproductive biomass, $R_i(t)$ (g.m⁻³.year⁻¹), was obtained from the total rate at which mass for reproduction was created at size x , integrated over x :

$$(A5) \quad R_i(t) = 0.5 \int (1 - E_i(x)) w_0 e^{x_{i,egg}} g_i(x, t) U_i(x, t) dx$$

with the factor 0.5 being an assumption that half of this mass contributes to eggs.

The predation death rate, $d_i(x, t)$ (year⁻¹), in the fish species balanced the mass consumed by predators. This also starts from

eq. A2, multiplying it by predator density, integrating over predator sizes x' and summing over predator types j :

$$(A6) \quad d_i(x, t) = A \sum_j \theta_{ji} \int e^{\alpha x'} \phi_j(x', x) U_j(x', t) dx'$$

The nonpredation death rate, $\mu_i(x, t)$ (year⁻¹), allowed for the existence of mortality other than predation. We followed a previous approach (Hall et al. 2006) that described this death rate as a U-shaped function of body size x :

$$(A7) \quad \mu_i(x, t) = \begin{cases} \mu_0 e^{-0.25(x-x_0)} & \text{for } x < x_{i,s} \\ \mu_{x_{i,s}} e^{k_i(x-x_{i,s})} & \text{for } x \geq x_{i,s} \end{cases}$$

For body sizes smaller than $x_{i,s}$ at which senescence started, a standard function was set for both species such that the death rate was μ_0 at x_0 , taking $\mu_0 = 0.2$ at $\exp(x_0) = 0.001$ g; the exponent -0.25 is a standard allometric scaling of the mortality rate to body mass (Brown et al. 2004). The death rate at the start of senescence ($\mu_{i,s} = \mu_i(x_{i,s}, t)$). From this size onwards, the death rate grew with an exponent $k_i = (\log(\mu_{i,\infty}/\mu_{i,s})) / (x_{i,\infty} - x_{i,s})$, where $x_{i,\infty}$ is the asymptotic body size to which type i grew, and $\mu_{i,\infty}$ is a maximum death rate shared by both species. It was assumed that $x_{i,s} = x_{i,\infty} - 1$. A time-independent form of $\mu_i(x, t)$ was used here.

Density dependence, $D_i(x, t)$, was needed to ensure that the density of each fish species i would not increase without limit, predation being insufficient in the case of these planktivores. We used a two-system species for simplicity. We introduced a density-dependent constraint in the egg production, drawing on the maximum density of eggs observed ($U_{i,egg}$) at sea during spring for each species from 2000 to 2006, and the density of eggs ($U_i(x_{i,egg}, t)$). We took a ratio $r_i(x, t) = U_i(x_{i,egg}, t) / 0.1 U_{i,egg}$ to construct a density-dependent function: $D_i(x, t) = e^{-cr_i(x, t)}$; the Dirac- δ function $b_i(x)$ in eq. A1 ensured that this applies only at egg size. The factor 0.1 assumes that the seasonal egg production is spread evenly over the whole year in this nonseasonal model.

Appendix B. Parameter values

Here we give the sources for species-independent and species-dependent parameter values used in the size-spectra model. Table B1 summarizes the species-dependent parameters. The initial conditions of the fish size spectra for the simulation experiments are shown in the last section of the Appendix B.

Species-independent parameters: size-spectrum dynamics

The feeding-rate constant (A), the exponent of mass in volume of water searched (α), and the food conversion efficiency (K) used in this study are $A = 640$ (m³.year⁻¹.g^{- α}), $\alpha = 0.8$, and $K = 0.1$ (Ware 1978), as in other size-spectrum models (Blanchard et al. 2009; Law et al. 2009; Andersen and Pedersen 2010; Datta et al. 2011; Hartvig et al. 2011). A value 0.2 for the scaling parameter ρ in the allocation to reproduction is thought to be appropriate (Law et al. 2012).

The value of $\mu_{i,\infty}$ in the nonpredation mortality was fixed for both species at a value of 10.year⁻¹, meaning that the nonpredation death rate rose to a maximum of 10.year⁻¹ at the asymptotic size. Fish species growing to larger body sizes were not included, and this extra mortality prevented an unrealistic build-up in density of big anchovy and sardine, which were largely invulnerable to predation in the absence of larger species.

A value of $c = 10$ in the density-dependence function was chosen such that after numerical integration of the model, the density of anchovy eggs in the model would be close to the observed densities of anchovy eggs in the 2008 survey of the NCME (Braun et al. 2009).

Table B1. Life history parameters of anchovy and sardine.

Parameter	Symbol	Anchovy	Sardine	Unit	Sources
Maturation parameters	$\varepsilon_{i,0}$	18.09	27.26		Canales and Leal 2009; Canales et al. 2003; Roa and Ernst 1999
	$\varepsilon_{i,1}$	1.45	1.02		
	$w_{i,egg}$	0.0003	0.0035	g	Castro et al. 2009; Hunter and Kimbrell 1980
Egg mass					
Growth parameters	$L_{i,\infty}$	20.25	38.60	cm	Cubillos 1991; Froese and Pauly 2000
	k_i	0.9	0.21	year ⁻¹	Canales and Leal 2009; Froese and Pauly 2000
	$t_{i,0}$	-0.01	-0.75	years	Canales and Leal 2009; Froese and Pauly 2000
	$w_{i,\infty}$	66.48	625.10	g	Cubillos 1991; Froese and Pauly 2000
Allometric parameters	a_i	0.0048	0.0068	g·cm ^{-b_i}	Fishery Data (IFOP)
	b_i	3.16	3.13		
Fish spectra: size range and initial conditions	$x_{i,egg}$	-8.2	-5.7		Castro et al. 2009; Hunter and Krimbell 1980
	$U_{i,egg}$	e ^{0.819}	e ^{-5.926}	m ⁻³	Braun et al. 2009

Note: Maturation parameters $\varepsilon_{i,0}$ and $\varepsilon_{i,1}$ describe maturity based on the body length. $L_{i,\infty}$, k_i , and $t_{i,0}$ are the asymptotic length, growth rate, and age at minimum length, respectively, from the von Bertalanffy somatic growth model. These models were used to be compared with somatic growth obtained from solving the size-spectrum model. Parameters a_i and b_i are from the allometric function between length (l) and weight (w) = $a_i l^{b_i}$ used to convert each species' asymptotic length to asymptotic weight ($w_{i,\infty}$) and reproduction function. Egg densities ($U_{i,egg}$) for each species in the survey of 2008 were used as initial values for the numerical simulations.

Species-dependent parameters: size-spectrum dynamics

Maturity ogive parameters for anchovy were taken from literature (Canales and Leal 2009). Maturity parameters for sardine were obtained by fitting empirical data (Canales et al. 2003) to a logistic function (Roa and Ernst 1999) of the form $P(l) = \frac{1}{1 + \exp(\varepsilon_{i,0} - \varepsilon_{i,1}l)}$, where $P(l)$ corresponds to the proportion of female mature at the body length (l), and $\varepsilon_{i,0}$ and $\varepsilon_{i,1}$ (Table B1) are parameters.

Parameters a_i and b_i (Table B1) came from fitting empirical data to the allometric relationship between length (l) and mass (w), $w = a_i l^{b_i}$. Data were provided by Institute of Fisheries Development - Chile.

The proportion of the mass allocated to reproduction for each fish species requires the asymptotic size ($x_{i,\infty}$) = $\log(W_{i,\infty}/w_0)$. For anchovy, the value was obtained using the allometric relationship $W_{i,\infty} = a_i L_{i,\infty}^{b_i}$ using the asymptotic length ($L_{i,\infty}$) (Cubillos 1991). For sardine, $W_{i,\infty}$ was available in Fishbase (Froese and Pauly 2000).

Mass of fish eggs ($x_{i,egg}$) for anchovy is shown in Table B1. Egg mass for sardine was calculated assuming a sphere of volume $V = \frac{4}{3}\pi\left[\frac{d}{2}\right]^3$ and transformed to mass assuming the density of water of 1 (g·m⁻³), the diameter (d) for sardine eggs being obtained from literature (Hunter and Kimbrell 1980).

Simulation experiments: initial conditions

Baseline spectra were given for the two fish species to provide initial conditions for numerical integration of the size-spectrum model. These spectra were assumed to follow a power law function of the form $U_i(x) = U_{i,egg}(x - x_{i,egg})^{\lambda_i}$, with $\lambda_i = -1$ (Sheldon et al. 1972; Marquet et al. 2005) (no data were available to estimate the slope). The numerical density of fish species i , $U_{i,egg}$ (m⁻³), at the egg size $x_{i,egg}$ was obtained from ichthyoplankton data (Braun et al. 2009). The total number of fish eggs in 10 m² was available by station. An averaged value for the area of study was estimated and expressed (in m⁻³) as 23.9 eggs·m⁻³. The proportion of sardine eggs was taken from the observations made between 2000 to 2006 (Braun et al. 2009). Egg densities of anchovy and sardine were calculated for this period based on their relative proportions. This period was considered a "normal" condition in the system, which means an absence of strong El Niño events.

Appendix C. Size structures of the plankton community

Plankton spectrum: cool conditions

From a monitoring survey carried out in October 2008 off northern Chile (Braun et al. 2009), data were selected for an

area 18°21'S–24°00'S and a depth range of 0 to 50 m to build the empirical plankton spectrum. From the data, the numerical density (m⁻³) of the following plankton groups was obtained: picoplankton (0.2–2 μm), nanoplankton (2–20 μm), microphytoplankton (20–200 μm), microzooplankton (20–200 μm), and zooplankton (>200 μm). Assumptions about the cell volume of each plankton group were needed to obtain the numerical density at a particular body mass of plankton (see last section). The volumes calculated for all groups were transformed into mass (g) with standard value 1 (g·cm⁻³) for water density. Body mass class (g) and density (m⁻³) were binned into log_e scales and the plankton spectrum was obtained.

Plankton spectrum: warm conditions

First, the slope (b), the intercept (a), and the cell mass that accounted for 50% and 80% of the total phytoplankton biomass (M_{B50} and M_{B90-10} , respectively) were predicted using the satellite CHL data. We used the following empirical relationships: (i) slope (b) = $-1.196 + 0.099\log_{10}(\text{CHL})$ (Barnes et al. 2011, table III); (ii) intercept (a) = $9.704 + 0.585\log_{10}(\text{CHL})$ (Barnes et al. 2011, table III); (iii) 50% of the total phytoplankton biomass (M_{B50}) = $0.748 + 1.215\log_{10}(\text{CHL})$ (Barnes et al. 2011, supplementary material, table 1), and (iv) 80% of the total phytoplankton biomass (M_{B90-10}) = $2.9 - 0.109\log_{10}(\text{CHL})$ (Barnes et al. 2011, supplementary material, table 1).

Second, the cumulative phytoplankton biomass was estimated as a function of cell size. This estimation was based on the cell masses at 0% (M_{B0}), 10% (M_{B10}), 90% (M_{B90}), and 100% (M_{B100}) given in Barnes et al. (2011, supplementary material).

Third, the biomass of the three phytoplankton groups (pico, nano, and micro) was obtained from equation $\int_{M_1}^{M_n} (bM + a) dM = \frac{1}{2}bM_n^2 + aM_n - \frac{1}{2}bM_1^2 - aM_1$ (Barnes et al. 2011, supplementary material), where M is cell mass, M_1 and M_n are the lower and upper boundaries, respectively (Barnes et al. 2011, supplementary material), of the pico-, nano-, and micro-plankton, and b and a are predicted slope and intercept, respectively (Barnes et al. 2011, table III). This gave time series for the biomasses of pico-, nano-, and micro-phytoplankton from 1997 to 2008.

Plankton spectrum: volume cells assumptions

Densities of the picoplankton and the five nanoplankton classes (2–4 μm, 4–8 μm, 8–12 μm, 12–16 μm, and 16–20 μm) were assigned to the midpoint of the class. Cell volume was found by assuming that cells were spheres with diameter (d) given by the

Can. J. Fish. Aquat. Sci. Downloaded from www.nrcresearchpress.com by 23.112.19.72 on 01/13/16 For personal use only.

midpoint size class. Thus, volume was calculated as $V = 4/3\pi r^3$, with $r = d/2$.

Microplankton density was available fractioned for the dominant species. Body volume of each species was taken from literature (Espinoza and Bertrand 2008). When cell volume of a genus was not available from literature, an average volume was calculated by the group (diatoms or dinoflagellates) and assigned to the species. This was the case for two dinoflagellate species.

Microzooplankton densities were also available for the six main dominant groups in the community (ciliates, copepodites, nauplii, eggs, radiolarians, and tintinnids). Body volumes (μm^3) for radiolarians and tintinnids were taken from literature (Espinoza and Bertrand 2008). Body mass (g) of copepodites and nauplii were taken from <http://earth.leeds.ac.uk/cyclops/data/ncfs-zooplank.xls>. Ciliates and eggs were assumed to be spherical. Measures of body size for these two groups were available from the same source of data, and the average diameter for each group was taken.

Zooplankton densities were fractioned into 12 size classes. An ellipsoidal shape ($V = 0.52d^2D$) of their volume was assumed (Echevarría and Rodríguez 1994), where the D is the length of the longest axis in the ellipsoid and d is the width of mean cross section assumed as $D/3$.

References for Appendices A, B, and C

Andersen, K.H., and Beyer, J.E. 2006. Asymptotic size determines species abundance in the marine size spectrum. *Am. Nat.* **168**, 54–61. doi:10.1086/504849.

Andersen, K.H., and Pedersen, M. 2010. Damped trophic cascades driven by fishing in model marine ecosystems. *Proc. R. Soc. B Biol. Sci.* **277**: 795–802. doi:10.1098/rspb.2009.1512.

Barnes, C., Irigoien, X., de Oliveira, J., Maxwell, D., and Jennings, S. 2011. Predicting marine phytoplankton community size structure from empirical relationships with remotely sensed variables. *J. Plankt. Res.* **33**: 13–24. doi:10.1093/plankt/fbq088.

Blanchard, J.L., Jennings, S., Law, R., Castle, M.D., McCloghrie, P., Rochet, M.-J., and Benoit, E. 2009. How does abundance scale with body size in coupled size-structured food webs? *J. Anim. Ecol.* **78**: 270–280. doi:10.1111/j.1365-2656.2008.01466.x. PMID:19120607.

Blanchard, J.L., Andersen, K.H., Scott, F., Hintzen, N.T., Piet, G., and Jennings, S. 2014. Evaluating targets and trade-offs among fisheries and conservation objectives using a multispecies size spectrum model. *J. Appl. Ecol.* **51**(3): 612–622. doi:10.1111/1365-2664.12238.

Braun, M., Reyes, H., Pizarro, E.M., Herrera, L., Santander, E., Claramunt, G., Oliva, E., Valenzuela, V., Castañi, V., Saavedra, J., et al. 2009. Monitoreo de las condiciones bio-oceanográficas entre la I y IV Regiones, año 2008. Fondo de Investigación Pesquera, Informe Final FIP/2008-21; www.fip.cl.

Brown, J.H., Gillooly, J.F., Allen, A.P., Savage, V.M., and West, G.B. 2004. Toward a metabolic theory of ecology. *Ecology*, **85**: 1771–1789. doi:10.1890/03-9000.

Canales, T.M., and Leal, E. 2009. Life history parameters of anchoveta, *Engraulis ringens* Jenyns, 1842, in central north Chile. *Rev. Biol. Mar. y Oceanogr.* **44**: 173–179. doi:10.4067/S0718-19572009000100017.

Canales, T.M., Saavedra, J. C., Böhm, G., and Martínez, C. 2003. Investigación CTP Anchoveta y Sardina III – IV Región, 2004. Informe Final. IFOP-SUBPESCA, Chile; www.ifop.cl.

Castro, L., Claramunt, G., Krautz, M., Llanos-Rivera, A., and Moreno, P. 2009. Egg trait variation in anchoveta *Engraulis ringens*: a maternal response to changing environmental conditions in contrasting spawning habitats. *Mar. Ecol. Prog. Ser.* **381**: 237–248. doi:10.3354/meps07922.

Cubillos, L. 1991. Estimates of monthly biomass, recruitment and fishing mortality of anchoveta (*Engraulis ringens*) off northern Chile in the period 1986–1989. *Biol. Pesq.* **20**: 49–59.

Datta, S., Delius, G., Law, R., and Plank, M.J. 2011. A stability analysis of the power-law steady state of marine size spectra. *J. Math. Biol.* **63**: 779–799. doi:10.1007/s00285-010-0387-z. PMID:21161230.

Echevarría, F., and Rodríguez, J. 1994. The size structure of plankton during a deep bloom in a stratified reservoir. *Hydrobiologia*, **284**: 113–124. doi:10.1007/BF00006883.

Espinoza, P., and Bertrand, A. 2008. Revisiting Peruvian anchovy (*Engraulis ringens*) trophodynamics provides a new vision of the Humboldt Current system. *Prog. Oceanogr.* **79**: 215–227. doi:10.1016/j.pocean.2008.10.022.

Froese, R., and Pauly, D. 2000. FishBase 2000: concepts, design and data sources. ICLARM, Los Baños, Laguna, Philippines.

Hall, S.J., Collie, J.S., Duplisea, D.E., Jennings, S., Bravington, M., and Link, J. 2006. A length-based multispecies model for evaluating community responses to fishing. *Can. J. Fish. Aquat. Sci.* **63**(6): 1344–1359. doi:10.1139/f06-039.

Hartvig, M., and Andersen, K.H. 2013. Coexistence of structured populations with size-based prey selection. *Theor. Popul. Biol.* **89**: 24–33. doi:10.1016/j.tpb.2013.07.003. PMID:23927897.

Hartvig, M., Andersen, K.H., and Beyer, J.E. 2011. Food web framework for size-structured populations. *Theor. Popul. Biol.* **272**: 113–122. doi:10.1016/j.jtbi.2010.12.006.

Hunter, J.R., and Kimbrell, C.M. 1980. Egg cannibalism in the Northern Anchovy, *Engraulis mordax*. *Fish. Bull.* **78**: 811–816.

Law, R., Plank, M.J., James, A., and Blanchard, J.L. 2009. Size-spectra dynamics from stochastic predation and growth of individuals. *Ecology*, **90**: 802–811. doi:10.1890/07-1900.1.

Law, R., Plank, M.J., and Kolding, J. 2012. On balanced exploitation of marine ecosystems: results from dynamic size spectra. *ICES J. Mar. Sci.* **69**: 602–614. doi:10.1093/icesjms/fss031.

Marquet, P.A., Quiñones, R.A., Abades, S., Labra, F., Tognelli, M., Arim, M., and Rivadeneira, M. 2005. Scaling and power-laws in ecological systems. *J. Exp. Biol.* **208**: 1749–1769. doi:10.1242/jeb.01588. PMID:15855405.

Roa, R., and Ernst, B. 1999. Estimation of size at sexual maturity: an evaluation of analytical and resampling procedures. *Fish. Bull.* **97**: 570–580.

Sheldon, R.W., Prakash, A., and Sutcliffe, W.H. 1972. The size distribution of particles in the ocean. *Limnol. Oceanogr.* **17**: 327–340. doi:10.4319/lo.1972.17.3.0327.

Ware, D.M. 1978. Bioenergetics of pelagic fish: theoretical change in swimming speed and ration with body size. *J. Fish. Res. Board Can.* **35**: 220–228. doi:10.1139/f78-036.